NPS-CS-96-010

NAVAL POSTGRADUATE SCHOOL
Monterey, California

Gait and Foot Trajectory Planning for Versatile Motions of a Six Legged Robot

by

Kan Yoneda
Kenji Suzuki
Yutaka Kanayama
Hidetoshi Takahashi
Junichi Akizono

October 1996

Prepared for: Naval Postgraduate School
Monterey, CA 93943

NAVAL POSTGRADUATE SCHOOL
Monterey, California

Rear Admiral M.J. Evans
Superintendent

R. Elster
Provost

This report was prepared for Naval Postgraduate School and funded by the National Science Foundation. Reproduction of all or part of this report is authorized.

This report is prepared by:

Yutaka Kanayama
Professor of Computer Science

Reviewed by:

Ted Lewis, Chair
Department of Computer Science

Released by:

David W. Netzer
Associate Provost and Dean of Research

REPORT DOCUMENTATION PAGE

Form Approved
OMB No. 0704-0188

1. AGENCY USE ONLY (Leave blank)	2. REPORT DATE	3. REPORT TYPE AND DATES COVERED
	01 October 1996	Technical Report, Feb.1992 - July 1995

4. TITLE AND SUBTITLE
Gait and Foot Trajectory Planning for Versatile Motions of a Six Legged Robot

5. FUNDING NUMBERS
N6227192WER0069

6. AUTHOR(S)
Kan Yoneda, Kenji Suzuki, Yutaka Kanayama
Hidetoshi Takahashi, and Junichi Akizono

7. PERFORMING ORGANIZATION NAME(S) AND ADDRESS(ES)
Naval Postgraduate School
Department of Computer Science
833 Dyer Road
Monterey, CA 93943-5118

8. PERFORMING ORGANIZATION REPORT NUMBER
NPSCS-96-010

9. SPONSORING/MONITORING AGENCY NAME(S) AND ADDRESS(ES)
National Science Foundation
Environmental & Ocean Systems Program
Washington, D.C. 20550

10. SPONSORING/MONITORING AGENCY REPORT NUMBER

11. SUPPLEMENTARY NOTES

12a. DISTRIBUTION/AVAILABILITY STATEMENT
Approved for Public release;
Distribution is unlimited

12b. DISTRIBUTION CODE

13. ABSTRACT *(Maximum 200 words)*

This paper deals with the problem of planning and controlling a radially symmetric six-legged walker on an uneven terrain when a smooth time-varying body motion is required. The main difficulties lie on the planning of gaits and foot trajectories. As for the gaits, this paper discusses the forward wave gait of a variable duty factor and a variable wave direction. With the commanded body motion, the maximum possible duty factor is computed using the speed limit of the leg swing motion. Guaranteeing this maximum duty factor contributes to obtain higher stability. We proved the "continuity" of this forward wave gait planning algorithm adds the versatility to gaits planned.

The foot trajectory planning algorithm dynamically generates a smooth foot trajectory as a function of the instantaneous body motions by modifying standard leg motion templates. The robot can negotiate an uneven terrain by modifying a vertical leg motion by a signal of tactile sensors on the foot. The experiments proved that the robot can successfully track smooth curves with body rotations on an uneven terrain, and thus proved the robustness of the algorithms.

14. SUBJECT TERMS
Walking Robot, Six-Legged Robot, Underwater Robot, Gait Planning
Foot Motion Planning

15. NUMBER OF PAGES
36

16. PRICE CODE

17. SECURITY CLASSIFICATION OF REPORT	18. SECURITY CLASSIFICATION OF THIS PAGE	19. SECURITY CLASSIFICATION OF ABSTRACT	20. LIMITATION OF ABSTRACT
UNCLASSIFIED	UNCLASSISFIED	UNCLASSIFIED	SAR

Gait and Foot Trajectory Planning for Versatile Motions of a Six Legged Robot *

Kan Yoneda
Department of Mechano-Aerospace Engineering
Tokyo Institute of Technology
2-12-1 Ookayama, Meguro, Tokyo 152, Japan
yoneda@mes.titech.ac.jp

Kenji Suzuki
Department of Electronics Engineering
The University of Electro-Communications
1-5-1 Chofugaoka, Chofu, Tokyo 182, Japan
suzuki@jaken.hmw.mhi.co.jp

Yutaka Kanayama
Computer Science Department
Naval Postgraduate School
Monterey, California 93943
kanayama@cs.nps.navy.mil
http://www.cs.nps.navy.mil/people/faculty/kanayama/

Hidetoshi Takahashi and Junichi Akizono
Machinery Division, Port and Harbour Research Institute,
Ministry of Transport
3-1-1 Nagase, Yokosuka, Kanagawa 239, Japan

*This work was supported by the National Science Foundation under grant BCS-9109989 and the Science and Technology Agency of Japan.

Abstract

This paper deals with the problem of planning and controlling a radially symmetric six-legged walker on an uneven terrain when a smooth time-varying body motion is required. The main difficulties lie on the planning of gaits and foot trajectories. As for the gaits, this paper discusses the forward wave gait of a variable duty factor and a variable wave direction. With the commanded body motion, the maximum possible duty factor is computed using the speed limit of the leg swing motion. Guaranteeing this maximum duty factor contributes to obtain higher stability. We proved the "continuity" of this forward wave gait planning algorithm adds the versatility to gaits planned.

The foot trajectory planning algorithm dynamically generates a smooth foot trajectory as a function of the instantaneous body motions by modifying standard leg motion templates. The robot can negotiate an uneven terrain by modifying a vertical leg motion by a signal of tactile sensors on the foot. The experiments proved that the robot can successfully track smooth curves with body rotations on an uneven terrain, and thus proved the robustness of the algorithms.

1 Introduction

A practical walking machine should be able to walk versatilely following a continuous curvature of the commanded locomotion trajectory. Especially, walking omnidirectionally on uneven terrain is an indispensable feature of legged machines. This research is related to a radially symmetric six legged robot, which has an advantage of having a uniform performance in an arbitrary crab angle.

A number of periodic gait planning methods for six-legged walker have already been proposed [1] – [10]. For six-legged robots, the *tripod* gait is the simplest periodic gait, in which two sets of tripods move alternately. Although the control method of this gait is simple, it is appropriate only at a specific speed as seen later. We want a more general gait planning algorithm which gives larger stability for a slower speed.

The (forward) wave gait for a longitudinally symmetric multi-legged robot is a gait in which a wave of lift-off events propagates forward along each side. Song and Waldron demonstrated that the wave gait provides the largest stability margin at any given duty factor on a longitudinally symmetric six legged walker [2]. It seems to have largest stability margin for a radially symmetric walker also [3]. This research issue was systematically investigated by Zhang and Song [4]. However, the conventional wave gait had limitations in at least two aspects. A larger duty factor means a larger stability margin. Therefore, we should use the maximum duty factor determined by the robot's commanded speed and the leg's maximum swing speed, which are generally variable over time. In the conventional wave gait, a duty factor is kept constant and cannot be changed when walking [2]. This is the first of the two limitations.

In order to obtain larger stability, it is essential for a walker to have its wave propagating direction equal to the desired crab angle when walking (A *crab angle* is the motion direction in the robot's coordinate system). However, it is not possible in the conventional wave gait to continuously change the wave propagating direction when walking. This is the second limitation. This capability of changing the wave propagation is needed for a walking robot to track a curved trajectory. Lee and Orin proposed a method to change the crab angle by using only two wave propagation directions: backward or forward [5]. However, in this gait, the wave propagation direction and crab angle are not the same and some hysteresis is unavoidable in the direction switching. A gait is said to be *semi-periodic* if its duty factor or relative phases are variable over time. In this paper, we will show a *variable parameter* gait planning algorithm which generates semi-periodic gaits with a variable speed, with a variable motion direction, and with a variable body rotation, answering the aforementioned research questions. More specifically, this algorithm embodies the best duty factor and the best combination of relative phases for each leg under a given motion command. The main theoretical results in this paper are explicitly stated in three Propositions. The computation time for this algorithm is much less than that for fully intelligent free gait planning algorithms [11] [12]. This algorithm generates not only the conventional wave gaits (such as tripod gaits), but other useful gaits as well.

As for the trajectory of a transferring foot, Lee and Orin [1, 5] described an algorithm for a foot to follow the body motion. They used a rectangle trajectory, which is not suitable for smooth foot motion. Sakakibara and Hirose proposed to use a smooth foot trajectory, in which the next foothold must be determined by the time of its lift-off. Hence, their algorithm cannot execute a curved body trajectory [13, 14]. The features of the foot trajectory planning algorithm investigated in this paper are (i) a smooth foot trajectory template is adopted, (ii) omni-directional motion commands are allowed, (iii) footholds are dynamically determined in order to deal with the omni-directional motions, and (iv) each foot velocity is dynamically evaluated because of the foothold point's possible motion. The algorithm stated here is the most general one among others reported so far, because the method by [5] satisfies (ii) and (iii), but not (i), and because the method given by [13, 14] satisfies (i), but neither (ii) nor (iii).

The activities described in this paper are related to the robot AQUAROBOT, which was constructed by the Port and Harbour Research Institute (PHRI), Ministry of Transport of Japan. PHRI has constructed three experimental six-legged underwater walking robots, AQUAROBOT, for underwater inspection tasks (Fig. 1). The second version was tested in a real enviroment. The task was to inspect the evenness of a rubble mound of size of 42×77 meters at an average depth of 24 meters in the caisson yard for Kamaishi Bay Breakwaters [16, 17].

This research was a part of the international cooperated research project administered mainly by the Naval Postgraduate School (NPS) in the US and PHRI [15]. The research activities in the US have been mostly supported by the National Science Foundation for three years beginning in February 1992. Activities in Japan have been partially supported by the Science and Technology Agency for the Japanese fiscal year of 1993 [18, 19]. One of the purposes of this research project was to improve the performance of these underwater walking

robots through international collaboration, and more specifically, to make its walking speed faster. An implementation of these algorithms was done on the AQUAROBOT system for evaluating their correctness and efficiency. The successful results proved not only the correctness, but a fact that the algorithms require only modest computation time to make real time control of the robot hardware possible. The research goals of this whole project also included linkage dynamics, virtual reality simulation model, and task and mission level control architecture [22, 23, 24].

2 Problem Statements and Overview of the Control System

The objective of this research is to find a leg motion planning algorithm for a radially symmetric walking robot to embody smooth continuous body motion commands on an uneven terrain with optimal stability. The input to this algorithm is a rigid body motion specification to the robot and the output is a description of foot motions. The difficulties of this problem lie in the fact that the gait must have larger stability for any situation, that the leg motion must be smooth and must negotiate a terrain roughness, that the body rotation may be superimposed on translational motion, that the body speed may change with a real-time command.

In order to solve the problem of realizing a versatile control algorithm as stated above, we propose a global hierarchical architecture of the control system as shown in Figure 2. The body motion description block provides a smooth body motion command to follow a path which specified for global robot tasks. Once the body motion command is given, the gait planning block generates a sequence of the legs' lift-off and touch-down events to produce a larger stability margin. A static stability margin on an uneven terrain is defined the same as that on a flat terrain. Thus, this gait planning algorithm is available also on an uneven terrain. The gait is specified by a duty factor and relative phases. Hence, the gait planning block has a function to decide a duty factor and relative phases based on the body motion command. The foot trajectory planning block generates a foot motion that allows the body to follow the commanded motion. It includes an uneven terrain negotiation algorithm. The foot motion is planned in the world coordinate system, and translated to the body coordinates to calculate joint angular rates.

3 Gait Planning

3.1 Principle

A body motion of a walking robot is basically described by six degrees of freedom, since the body moves in the three dimensional space. However, in order to make the problem simpler, we assume that its height z is constant, and its pitch and roll angles are null. Thus,

the robot's motions are confined in a horizontal plane. Therefore, in this paper, a *motion command* is given by

$$\mathcal{Q}(t) = \Big(v(t), \theta(t), \omega(t)\Big), \tag{1}$$

where $v(t)$ (≥ 0) is the horizontal translational motion speed, $\theta(t)$ the horizontal translational motion direction, and $\omega(t)$ the rotational velocity (about z axis) of the robot respectively [25]. This (instantaneous) motion command $\mathcal{Q}(t)$ is the input to the gait planning algorithm; the output is a set of up-and-down timings of the leg expressed by a duty factor $\beta(t)$ and relative phases $\psi_i(t)$ for leg i.

Since v, θ and ω are variables of time, the motion speed may be changing, the motion trajectory may be curved, and the robot's heading direction may not be equal to its motion direction $\theta(t)$. Therefore, the problem of optimizing the stability all the time is not trivial.

In order to solve this problem of maximizing stability, a new concept of *variable parameter* forward wave gait is introduced. In a regular gait [6], the *duty factor* $\beta(t)$ is the ratio of the supporting interval to the cycle time. We first find the maximum duty factor $\beta_{\max}$ for a given motion command $\mathcal{Q}(t)$. Next, we embody this maximum duty factor $\beta_{\max}$ by continuously changing $\beta(t)$. This method works to obtain larger stability.

A *crab angle* $\alpha(t)$ is the difference between the robot's heading (direction of leg 1) and body motion direction $\theta(t)$. The *relative phase* ψ_i of leg i is the touch-down instance normalized by one cycle time. The legs are numbered as shown in Figure 3. A crab angle α divides the six legs into two groups: left and right. (In a special case where the body motion direction equals to the direction of one leg, assume that both left and right leg groups include the forefront and rearmost legs.) A *forward wave gait* for a radially symmetric walking robot is defined as a gait in which the wave of touch-down events propagates forward in each group, and the phase difference between the neighbors in each group is $1 - \beta$. That means when one leg touches-down, the next one is lifted-off. In the conventional forward wave gait, the phase difference between two groups is $1/2$ so that the two legs in a longitudinally symmetric positions move alternately each other. However, in a radially symmetric walker, the phase difference between two groups may not be necessarily equal to $1/2$. The gait planning algorithm developed here generates the conventional forward wave gait as a special case where $\alpha(t) = (2n-1)\pi/6$. No jerky motion occurs in any case, because the gait generator function is continuous.

When the body motion direction changes over time, we continuously change the wave propagating direction so that both of directions become equal. This method also contributes to obtain larger stability.

A regular/periodic gait is normally described by a duty factor β and a set $\langle \psi_1, \cdots, \psi_6 \rangle$ of relative phases, which are constant over time. However, in this paper, the duty factor $\beta(t)$ and the relative phases $\psi_i(t)$ are functions of time and defined more generally as follows. A variable parameter forward wave gait is a collection of regular and periodic *reference* gaits $\mathcal{G}(t)$. That means, at each given time t_1, the gait $\mathcal{G}(t_1)$ is a regular/periodic gait. Its duty factor $\beta(t_1)$ and relative phases $\psi_i(t_1)$ are defined as ones of the instantaneous reference regular/periodic gait $\mathcal{G}(t_1)$. Other instantaneously definable values, such as positions and

velocities of the legs, are also those of the reference gait.

Under this variable parameter forward wave gait planning method, we define a *gait generator* $\Psi_i (i = 1, \cdots, 6)$ of a crab angle $\alpha(t)$ and a duty factor $\beta(t)$ to obtain a relative phase $\psi_i(t)$ of leg i:

$$\psi_i(t) = \Psi_i\big(\alpha(t), \beta(t)\big) \qquad i = 1, \ldots, 6 \tag{2}$$

A gait generator Ψ_i must be a continuous function of $\alpha(t)$ and $\beta(t)$ in order to obtain dynamically changing gaits when the parameters $\alpha(t)$ and $\beta(t)$ change. A discontinuity in a relative phase causes jerky leg motion. For instance, if Ψ_i is discontinuous, a free leg may need to become a support one instantaneously, even when the leg is still horizontally moving.

3.2 Maximum Duty Factor

In a regular gait without rotation, an average velocity of

$$u(t) = \frac{\beta(t)}{1 - \beta(t)} v(t) \tag{3}$$

is required for a swing leg [14], where $\beta(t)$ is a duty factor and $v(t)$ its motion speed. The duty factor defined in Section 3.1 is still valid for a variable parameter gait. In a motion with a translational component $v(t)$ and a rotational component $\omega(t)$, the average velocity $u(t)$ at the outermost leg is

$$u(t) = \frac{\beta(t)}{1 - \beta(t)} \big(v(t) + |\omega(t)|\, R\big), \tag{4}$$

where R is the distance from the body center to the outermost point of a leg's constrained working area. If $U_{\max}$ denotes the maximum swing velocity,

$$\beta(t) = \frac{u(t)}{v(t) + |\omega(t)|\, R + u(t)} \leq \frac{U_{\max}}{v(t) + |\omega(t)|\, R + U_{\max}} \equiv \beta_{\max}(t), \tag{5}$$

where $\beta_{\max}(t)$ denotes the maximum duty factor. This value $\beta_{\max}(t)$ is the upper limit of the duty factor for any foot position [19]. From now on, we try to realize this velocity-dependent maximum duty factor $\beta_{\max}(t)$ all the time in order to obtain the maximum stability.

3.3 Varying the Duty Factor

Now we want to find a set of relative phases of all six legs satisfying the maximum duty factor $\beta_{\max}(t)$ given by Equation (5) so as to optimize the stability margin. We first consider the case in which the crab angle $\alpha = \pi/6$ and the commanded velocity is changing. Namely, we will find the function value $\Psi_i(\pi/6, \beta)$ in this Section.

Figure 4 shows the conventional wave gait diagram for $\beta = 5/6,\ 2/3$, and $1/2$. In order to find a continuous function $\Psi_i(\pi/6, \beta)$ with $1/2 \leq \beta \leq 2/3$, we design a gait pattern shown in

Figure 5. The upper and lower solid segments of each leg show a support phase at $\beta = 2/3$ and $\beta = 1/2$ respectively. The segments for $\beta = 1/2$ in Figure 5 were shifted by a $1/4$ phase from those in Figure 4 in order to minimize the total amount of the phase variations between two cases. By linearly interpolating these two segments, the relative phase for an arbitrary duty factor $\beta \in [1/2, 2/3]$ is obtained as shown by the broken line segments in the Figure.

Furthermore, by linear extrapolation, we simply obtain a gait generator set Ψ_i as

$$\Psi_i(\tfrac{\pi}{6}, \beta) = \Big[6\Big((\beta - \tfrac{1}{2})\Psi_i(\tfrac{\pi}{6}, \tfrac{2}{3}) - (\beta - \tfrac{2}{3})\Psi_i(\tfrac{\pi}{6}, \tfrac{1}{2})\Big)\Big]_{\mathrm{mod}1} \qquad (i = 1 \text{ to } 6) \tag{6}$$

for the full duty factor range of $(0, 1]$. Thus, the relative phase ψ_i for $\alpha = \pi/6$ is found as a linear continuous function of β. This gait class is shown in Figure 6.

Proposition 1 *There exists a continuous gait generator Ψ_i of β such that $\Psi_i(\pi/6,\ \beta)$ is a forward wave gait for any duty factor $\beta \in (0, 1]$.*

Proof. Since $\alpha = \pi/6$, the left leg group is $\langle 5,\ 6,\ 1\rangle$ and the right leg group is $\langle 4,\ 3,\ 2\rangle$ from the rear to the front respectively. Consider the gait class shown in Figure 6 and Equation (6). The touch-down timing of leg 5 is equal to the lift-off timing of leg 6, and the tough-down timing of leg 6 is equals to the lift-off timing of leg 1 for any duty factor. The same relation holds in the other side. The phase differences of the touch-down timings of leg pairs $\langle 1,\ 2\rangle$, $\langle 6,\ 3\rangle$, and $\langle 5,\ 4\rangle$ are $1/2$ respectively. Thus, the gaits generated by Equation (6) are forward wave gaits. ∎

Figure 7 shows supporting leg combinations at a kinematic phase ϕ (a time normalized by one cycle time) [1] for a given duty factor β. During its motion, a robot's state corresponds to a point with the current β and ϕ in the chart. If a robot is walking at a constant translational speed v without rotation, the robot's state moves along the horizontal line at the duty factor β given by Equation (5). In a special case of $\beta = 1/2$, this extended wave gait becomes the well-known tripod gait. When the robot increases its current translational speed $v(t)$, the current duty factor $\beta(t)$ decreases according to Equation (5) and the robot's state moves downward in this chart as its kinematic phase proceeds.

A gait with a duty factor $\beta < 1/2$ is statically unstable for a six legged walker. However, some of these gaits are still stable for a walker with more than six legs.

3.4 Varying the Crab Angle

In this Section, we are finding a wave gait planning method when its crab angle $\alpha(t)$ is variable. We first plan gaits for a variable crab angle $\alpha(t)$ with a fixed duty factor $\beta = 2/3$. In Figure 8, for each leg, the upper line segment shows its supporting interval with $\alpha = \pi/6$, and the lower line segment with $\alpha = -\pi/6$ ($\beta = 2/3$ in both cases). By interpolating these two segments, we obtain a gait for an arbitrary intermediate crab angle. This intermediate gait should also be classified into a forward wave gait, because a wave of lift-off events propagates forward.

For this fixed duty factor, it is straightforward to obtain a gait with a crab angle in the expanded range of $[0, 2\pi)$ taking into account of hexagonal symmetry. Figure 9 shows the relative phase function $\Psi_i(\alpha, \beta)$ for $\beta = 2/3$ and $\beta = 1/2$. These functions are explicitly described as follows:

$$\begin{aligned}
&\text{For } i = 1, 3, 5, \\
&\Psi_i(\alpha, \tfrac{2}{3}) = \begin{cases} \alpha'/(2\pi) & (\quad 0 \le \alpha' < 2\pi/3), \\ 1/3 & (2\pi/3 \le \alpha' < \pi), \\ -\alpha'/(2\pi) + 5/6 & (\quad \pi \le \alpha' < 5\pi/3), \\ 0 & (5\pi/3 \le \alpha' < 2\pi), \end{cases} \\
&\Psi_i(\alpha, \tfrac{1}{2}) = 1/4. \\
&\text{For } i = 2, 4, 6, \\
&\Psi_i(\alpha, \tfrac{2}{3}) = \begin{cases} \alpha'/(2\pi) + 1/2 & (\quad 0 \le \alpha' < 2\pi/3), \\ 5/6 & (2\pi/3 \le \alpha' < \pi), \\ -\alpha'/(2\pi) + 1/3 & (\quad \pi \le \alpha' < 5\pi/3), \\ 1/2 & (5\pi/3 \le \alpha' < 2\pi), \end{cases} \\
&\Psi_i(\alpha, \tfrac{1}{2}) = 3/4, \qquad (7)
\end{aligned}$$

where,

$$\alpha' = \left[\alpha - \frac{(2i-1)\pi}{6}\right]_{\text{mod } 2\pi} \qquad (8)$$

Proposition 2 *There exists a continuous gait generator Ψ_i of α such that $\Psi_i(\alpha,\ 2/3)$ is a forward wave gait for any crab angle $\alpha \in [0, 2\pi)$.*

Proof. Consider the class of gaits shown in Figure 9 and Equation (7). The touch-down events propagate from the rear to the front for any crab angle, and the phase lag of each leg to the neighboring one is $1/3$. The phase differences of left and right legs are $1/2$ for $\alpha(t) = (2n-1)\pi/6$. Thus, the gaits generated by Equation (7) are forward wave gaits. 2

Now we consider the cases in which the duty factor is also variable. In order to plan a gait for an arbitrary combination of α and β, we combine the algorithm described in Section 3.3 and the previous result (7). By substituting each occurrence of $\pi/6$ in Equation (6) by α, we obtain

$$\Psi_i(\alpha, \beta) = \left[6\Big((\beta - \tfrac{1}{2})\Psi_i(\alpha, \tfrac{2}{3}) - (\beta - \tfrac{2}{3})\Psi_i(\alpha, \tfrac{1}{2})\Big)\right]_{\text{mod } 1} \qquad (i = 1 \text{ to } 6), \qquad (9)$$

where $\Psi_i(\alpha, \frac{2}{3})$ and $\Psi_i(\alpha, \frac{1}{2})$ are obtained by Equation (7). That is, this algorithm generates a linear inter/extrapolation for both parameters of a crab angle and a duty factor.

Proposition 3 *There exists a continuous gait generator Ψ_i of α and β such that $\Psi_i(\alpha,\ \beta)$ is a forward wave gait for any crab angle $\alpha \in [0, 2\pi)$ and for any duty factor $\beta \in (0, 1]$.*

Proof. Consider the class of gaits given by Equation (9). The phase lag of each leg to the neighboring one is $1/3$ in $\Psi_i(\alpha, \frac{2}{3})$, and is $1/2$ in $\Psi_i(\alpha, \frac{1}{2})$ as demonstrated in Proposition 2. By substituting these values for $\Psi_i(\alpha, \frac{2}{3})$ and $\Psi_i(\alpha, \frac{1}{2})$, we find the total phase lag being $1 - \beta$. That means the gaits generated by Equation (9) are forward wave gaits. ∎

Figure 10 shows the supporting leg combination for a crab angle $\alpha = 0$. Compare this result with Figure 7.

3.5 Gait Examples

Figure 11 shows an example of a gait generated for a fixed crab angle and variable duty factor. The lines in the top part indicate the supporting phases the legs. The horizontal coordinate means time. The symbols in the lower part indicate positions and postures of the robot at a constant interval. The locomotion speed increases as the robot moves to the right. The duty factor decreases and the cycle time of the gait decreases as the speed increases. For any duty factor, the lift-off events propagate from the rear to front as the arrows show.

Figure 12 shows an example of a gait generated for a variable crab angle and a fixed duty factor. The hatched arrows indicate the correspondence between robot positions and leg states. The locomotion speed is constant in this case. The crab angle is $\pi/3$ at first, then is changed to zero, and finally becomes $-\pi/3$. For any crab angle, the lift-off events propagate from the rear to front as the arrows show.

The *stability margin* [8] is defined as the ratio C/D, where C is the horizontal distance between the body center and the nearest edge of the convex hull formed by the supporting feet, and D is the horizontal distance from the body reference point to a foot in the standard posture of the robot. Figure 13 shows the stability margins obtained by simulation for three distinct cases. The first one shown in a solid line is the result for a variable parameter forward wave gait along a circular path with a constant body orientation in the world coordinate system (a variable crab angle gait). The second one shown in a broken line is the result for a classical forward wave gait with $\alpha = \pi/6$ along a straight path. The third one shown in a dotted line is the result for a backward wave gait along a straight path. Notice that the stability margin of variable parameter forward wave gaits and that of fixed crab angle forward wave gaits are not much different and they are significantly better than that of backward wave gaits. This observation is consistent with what was proved on a longitudinally symmetric walker [2].

4 Foot Trajectory Planning

4.1 Objectives

The problem of foot motion planning for a walking robot is, given its gait, determining appropriate trajectories of the feet in the space to embody the gait.

The inputs to the algorithm are the body motion command, gait parameters such as β and ψ_i, and the robot's state variables such as the phase variables, foot positions and foot speeds. Notice that these inputs are dynamic. The outputs are commanded speeds to the joints. Therefore, this algorithm obtains optimal foot motions at every sampling time in a time-varying body commanded motion. After defining fundamental concepts in foot motion planning, we describe desirable properties for foot motions and next we design an algorithm to plan such kind of foot trajectories.

4.2 Computing Phase Variables

Evaluating phase variables is essential in the periodic behavior of a walking robot. The method described in this Section is based on the work by Lee and Orin [5].

The concept of the *constrained working volume* (CWV in short) of a leg is essential in foot trajectory design [5]. This concept was introduced to analyze interference among legs and to implement the spatial aspect of semi-periodic gait [5]. Generally the reachable volumes of all the feet of a robot overlap each other. In this paper, a cylindrical subset of the reachable volume of a leg is defined as the CWV of the leg in such a way that the CWVs of any two legs do not have intersections (the radius of the cylinder is r_{cwv}). This decision makes the foot trajectory computation task simpler.

The *temporal kinematic margin* t_{Si} of leg i is a predicted time-to-go until the foot-tip of leg i in the support phase reaches the surface of the CWV with the present foot velocity. By this definition [5],

$$t_{Si} = \frac{d}{|\boldsymbol{v}_{Fi}|}, \tag{10}$$

where $\boldsymbol{v}_{Fi}$ is the present foot velocity of leg i relative to the body and d is the distance from the support point to the surface of the CWV in the direction of $\boldsymbol{v}_{Fi}$. The kinematic period τ is given by [5]

$$\tau = \frac{1}{\beta} \min_i \left\{ \frac{t_{Si}}{1 - \phi_{Si}} \right\}. \tag{11}$$

The *leg phase variable* ϕ_{Li} which determines the phase of the leg i is defined as [5]:

$$\phi_{Li} = [\phi - \psi_i]_{\text{mod}1}, \tag{12}$$

where,

$$\begin{aligned} 0 \le \phi_{Li} < \beta \quad & \text{support phase,} \\ \beta \le \phi_{Li} \le 1 \quad & \text{transfer phase.} \end{aligned}$$

The *support phase variable* $\phi_{Si} \in [0, 1]$of leg i, which represents the phase during its support phase, being 0 at the touchdown and 1 at the lift-off is computed as follows [5]:

$$\phi_{Si} = \frac{\phi_{Li}}{\beta}. \tag{13}$$

The *transfer phase variable* $\phi_{Ti} \in [0, 1]$ of leg i, which represents the phase during its transfer phase, being 0 at the lift-off and 1 at the touchdown is computed as follows [5]:

$$\phi_{Ti} = \frac{\phi_{Li} - \beta}{1 - \beta}. \tag{14}$$

4.3 Transfer Phase: Trajectory Design

This Section discusses a foot motion planning algorithm in the period while a foot is moving (or transferring). A foot trajectory is a curve in the three-dimensional space and there exist tremendous number of distinct curve classes for our purpose. We specifically selected a trajectory class for foot motions which satisfies the following requirements.
(i) Trajectories are smooth so that acceleration of legs is easier for the motor controllers and foot motions would not give bad reactions to the body.
(ii) Trajectories have vertical portions at landing and leaving periods in order not to cause horizontal slippage of the feet.
(iii) Vertical foot motions at landing must be decelerated in order to reduce the landing impacts [13, 14].
(iv) Omni-directional body motions must be embodied.
(v) Each foot trajectory is constrained in a vertical flat plane named called a *foot trajectory plane* to simplify the trajectory design task.
(vi) Each trajectory (in a trajectory plane) is generated by a *foot trajectory template* to make the generation task easier. Because of Requirement (i), the trajectory template must also be smooth.
As we see later, we found these requirements were effective to control the robot in real time and to make the resultant motions smooth and natural.

We adopted a trajectory which satisfies the previous requirements in Figure 14, Part (a). Part (b) shows the vertical and horizontal velocities to generate the trajectory. A foot trajectory instance is generated depending on each dynamic situation on the current trajectory plane based on the trajectory template.

Let $\phi_{Ti} \in [0, 1]$ denote the *transfer phase variable* of leg i, which represents the phase during its transfer phase, 0 at the lift-off time and 1 at the touch-down time. This variable ϕ_{Ti} describes each foot motion as shown in Figure 14, Part (b). The *horizontal velocity* ξ_H and *vertical velocity* ξ_V are normalized.

As a part of foot trajectory planning task, each leg's next precise foothold position should be evaluated at each sampling time. The foothold position determines the foot trajectory instance. The next foothold position should be determined in relation to the motion of CWV.

First, we find the horizontal velocity of foothold position on X_W-Y_W plane. Let ${}^W\boldsymbol{p}_{Li} = (p_{Lix}, p_{Liy}, p_{Liz})^T$ be the CWV center of leg i in the world coordinate system, and ${}^W\boldsymbol{v}_{Li} = (v_{Lix}, v_{Liy}, v_{Liz})^T$ be the velocity of the CWV center in the world coordinate system. The predicted foothold ${}^W\boldsymbol{p}_{FHi} = (p_{FHix}, p_{FHiy}, p_{FHiz})^T$ in the world coordinate system is computed

as the intersection of the edge of the CWV and the ray drawn from the CWV center in the ${}^{W}\boldsymbol{v}_{Li}$ direction. Therefore, at the end of the transfer phase($\phi_{Ti} = 1$), the predicted foothold position will be

$$p_{FHix} = p_{Lix} + (1 - \phi_{Ti})\tau_T v_{Lix} + \frac{r_{\text{cwv}} v_{Lix}}{\sqrt{v_{Lix}^2 + v_{Liy}^2}}, \tag{15}$$

$$p_{FHiy} = p_{Liy} + (1 - \phi_{Ti})\tau_T v_{Liy} + \frac{r_{\text{cwv}} v_{Liy}}{\sqrt{v_{Lix}^2 + v_{Liy}^2}}, \tag{16}$$

where τ_T is the transfer period.

4.3.1 Negotiation with Uneven Terrain

Next, let us discuss the issue of how to negotiate with uneven terrains. We first assume that the robot's terrain is globally flat and there exists a local variance in the vertical unevenness of $\pm h$. The average height of the terrain is called the *ground level*, where $z = z_0$. To adapt this much terrain roughness, vertcal component of a foothold position is initially planned at a hight below the ground level by h. In a real robot's operation, the phase of a foot is switched from a transfer to support phase when its tactile sensor sends a signal. By this feedback mechanism, the robot can negotiate an uneven terrain.

$$p_{FHiz} = \begin{cases} z_0 - h, & \text{for } 0 \le \phi_{Ti} < \phi_1, \ \phi_2 \le \phi_{Ti} < \phi_3, \\ z_0 - H_L, & \text{for } \phi_1 \le \phi_{Ti} < \phi_2, \\ z_0 + h, & \text{for } \phi_3 \le \phi_{Ti} < 1, \end{cases} \tag{17}$$

where ϕ_1, ϕ_2 and ϕ_3 are the phases when a foot reaches a height of h, a clearance height of H_L and a height of $-h$ respectively (Figure 14).

So far we consider environments in which the ground is globally horizontal with the ground level of z_0 even though there is a small disturbance of $\pm h$. If a terrain is globally not horizontal, we propose the following method to negotiate it.
A local terrain is approximated by a plane

$$z = Ax + By + C, \tag{18}$$

where A, B, and C are constant. These are computed by the latest three supporting foot positions. Then the current terrain's height z_0 is dynamically evaluated as

$$z_0 = Ap_{Fix} + Bp_{Fiy} + C. \tag{19}$$

Since the robot can negotiate the unevenness of $\pm h$ from this variable z_0, it can walk on a slope as well with a semi-periodic gait.

4.3.2 Dynamic Trajectory Planning

If the robot is steadily walking at a constant speed and a direction, the trajectory plane of each foot has the same direction as the body translation direction, and the stride and

trajectory of each foot are the same. However, if the motion commands are changing, the trajectory plane may be bent and may be shrunk or stretched to coordinate with the commanded motions. The directions of the trajectory planes are not equal. The strides and speeds of all legs may not be equal anymore. Such an algorithm is needed to embody omni-directional body motions. This capacity is implemented by calculating an appropriate foot speed as described below.

When a body motion command is a variable over time, a foot trajectory needs to be expanded or shrunk elastically and this is possible through changing the coefficients ξ_H, ξ_V of trajectory templates. Hence the foot velocity ${}^W\boldsymbol{v}_{Fi}$ of leg i at the foot position of ${}^W\boldsymbol{p}_{Fi} = (p_{Fix}, p_{Fiy}, p_{Fiz})$ in the world coordinate system becomes

$$ {}^W\boldsymbol{v}_{Fi} = \begin{bmatrix} \frac{p_{FHix} - p_{Fix}}{\tau_T \int_{\phi_{Ti}}^{1} \xi_H(\phi')d\phi'} \xi_H(\phi_{Ti}) \\ \frac{p_{FHiy} - p_{Fiy}}{\tau_T \int_{\phi_{Ti}}^{1} \xi_H(\phi')d\phi'} \xi_H(\phi_{Ti}) \\ \frac{p_{FHiz} - p_{Fiz}}{|\tau_T \int_{\phi_{Ti}}^{\phi_e} \xi_V(\phi')d\phi'|} \xi_V(\phi_{Ti}) \end{bmatrix}, \tag{20} $$

where

$$ \phi_e = \begin{cases} \phi_2, & \text{for } 0 \le \phi_{Ti} < \phi_2 \\ 1. & \text{for } \phi_2 \le \phi_{Ti} < 1 \end{cases} . \tag{21} $$

The foot speed represented in the world coordinate system is converted into the body coordinate system and next translated into robot-dependent joint velocities using an inverse Jacobian matrix.

$$ {}^B\boldsymbol{v}_{Fi} = {}^B_W R({}^W\boldsymbol{v}_{Fi} - {}^W\boldsymbol{v} - {}^W\boldsymbol{\omega} \times {}^W\boldsymbol{p}_{Fi}), \tag{22} $$

where ${}^B_W R$ is the rotation matrix from the world to the body coordinate system [26].

$$ \dot{\boldsymbol{\Theta}}_i = \boldsymbol{J}^{-1}(\boldsymbol{\Theta}_i)\ {}^B\boldsymbol{v}_{Fi} \tag{23} $$

where $\boldsymbol{\Theta}_i = [\theta_1, \theta_2, \theta_3]$ is joint angules of each leg, and its derivative $\dot{\boldsymbol{\Theta}}$ is joint angular velocities. This final joint angular velocities are applied to the actuators.

4.4 Support Phases

In a support phase, a foot must move in such a way that the body makes continuous motion as specified by the command. The supporting foot position for each leg in the world coordinate system is assumed stationary during its support phase. Therefore, the foot velocity ${}^W\boldsymbol{v}_{Fi}$ relative to the body is represented as

$$ {}^B\boldsymbol{v}_{Fi} = {}^B_W R({}^W\boldsymbol{v}_{Fi} - {}^W\boldsymbol{v} - {}^W\boldsymbol{\omega} \times {}^W\boldsymbol{p}_{Fi}), \tag{24} $$

where ${}^B_W R$ is the rotation matrix from the world to the body coordinate system [26]. This last velocity is used to compute the joint angular velocity of each leg using an inverse Jacobian. In a real experiment, a foot detects its landing by a touch sensor and changes its state from transfer to supporting. By this method, the robot can adapt to an uneven terrain.

4.5 Foot Trajectory Example

Figure 15 shows a simulation result of an execution using this trajectory planning algorithm. In this Figure, the robot translates along a circular path with a constant body orientation. Each foot trajectory is incrementally generated from the trajectory template with enlarging or shrinking. This result demonstrates how dynamic leg motion planning and execution is done to embody a body motion command with rotation.

5 Experimental Results

This Section describes implementation results of the body motion, gait, and foot motion planning algorithms (Sections 3, and 4) on the robot system.

5.1 Description of the Robot System

The Port and Harbour Research Institute has constructed three models of six legged underwater walking robots. This series of experiments has been conducted on the first model. The AQUAROBOT hardware system consists of a main body and six radially symmetrically located legs. Each leg, made of anti-corrosive aluminum, has three degrees of freedom. The axis of the first joint is vertical and those of the second and third joints are horizontal. A disk-shaped foot is connected through the bottom limb of a leg through a passive spherical joint. One tactile sensor is attached to each foot. Each side of the hexagonal body is 30 centimeters long. The limbs of a leg are 14, 25, and 60 centimeters in length respectively. The motors for the second and third joints are mounted inside the limbs and, through harmonic gears and bevel gears, directly drive the limbs. This design allows their weights to be distributed over legs and makes water-tight structures easy. The powers of the first, second, and third motors are 80, 120, and 120 watts respectively. The total weight of AQUAROBOT in the air is 280 kilograms.

The control computer is an NEC PC-9821Xt/C10W based on a Pentium/90MHz CPU. The software system was written in C++. The sampling time is 50 milliseconds.

5.2 Variable Duty Factor

Figure 16 shows the snap shots of the walking experiment in which locomotion speed increases from Parts (a) to (c). Thus, the duty factor decreases. The line on the floor shows that the robot walks from right to the left. In Part (a), duty factor is about 1/6, and only ♯2 leg (left behind) is in the air. In Part (b), duty factor is about 2/6, and ♯1 and ♯3 legs are in the air. In Part (c), duty factor is about 3/6, and ♯2, ♯4 and ♯6 legs are in the air. The number of legs in the air is increased to produce a higher speed locomotion.

5.3 Variable Crab Angle

Figure 17 shows the snap shots of the walking experiment in which crab angle increases from Parts (a) to (b). The line on the floor shows that the robot walks from right to the left, and the direction of the leg ♯1 (white shank) shows that the robot rotates counter-clockwise in the top view. In Part (a), ♯3 and ♯5 legs are in the air. In Part (b), ♯1 and ♯3 legs are in the air. Thus, ♯3 leg is paired with ♯5 in Part (a) and with ♯1 in Part (b). The variation of the leg combination is planned to make a highly stable gait.

5.4 Walking on an Uneven Terrain

Figure 18 shows that AQUAROBOT is stably walking on an unknown uneven terrain. This motion was generated by the method described in Equation (20). The foot is able to step on and off an obstacle with a height of 10 centimeters. A comparison between the foot motions in Figures 15 and 18 demonstrates that the foot motion algorithm absorbs differences in foot holding height. Although the current control system does not include a body posture stabilizing feedback using an inclinometer, experiments of walking over an uneven terrain worked perfect as long as the walking path is not very long.

Through our prior experiments, we understand that the stability of a walking robot often fails by an elevation error of a landing point or a time lag of touchdown; because it causes an inclination of the body, especially when fewer legs are supporting the body. A larger stability margin and more supporting legs obtained by the new algorithm make the robot's performance better even in the disadvantageous condition. The correctness and effectiveness of the algorithms were thus demonstrated through these experiments.

6 Conclusions

The body and foot motion planning algorithms investigated here handles variable speeds, variable crab angles, and motion commands with superimposed rotation cases perfectly. This algorithm has a striking feature in that it always maximizes number of supporting legs in each situation. Thus, a large stability margin is obtained. The foot trajectory planning algorithm can deal with dynamic situations due to versatile commanded motions.

Correctness and effectiveness of the body/foot motion planning algorithms were proven by implementing them on AQUAROBOT. The robot walked smoothly with a variable speed and crab angle on a smooth curved commanded path. The foot motion planning algorithm for an uneven terrain was also proven successful.

Acknowledgments

We are thankful to Mineo Iwasaki, Shigeki Shiraiwa, Katsuei Nakagawa, and Toshinari Tanaka for their hardware and software system support. We also thank to Robert B. McGhee for his valuable comments.

References

[1] W. J. Lee and D. E. Orin, "The Kinematics of Motion Planning for Multilegged Vehicles Over Uneven Terrain," *IEEE Journal of Robotics and Automation,* vol. 4, no. 2, pp. 635-642, April 1988.

[2] S. M. Song and K. J. Waldron, *Machines That Walk: The Adaptive Suspension Vehicle,* The MIT Press, Cambridge, Massachusetts, 1989.

[3] K. Oohashi and K. J. Waldron, "Stability of a Six-Legged Walking Machine with an Axis-Symmetrical Leg Configuration," *Proc. of 10th Applied Mechanisms Conference.*

[4] C.D.Zhang and S.M Song, "A Study of the Stability of Generalized Wave Gaits" *Mathematical Biosciences,* vol. 115, no.1, pp. 1-32, 1993.

[5] W. J. Lee and D. E. Orin, "Omnidirectional Supervisory Control of a Multilegged Vehicle Using Periodic Gaits," *IEEE Journal of Robotics and Automation,* vol. 4, no. 6, pp. 635-642, December 1988.

[6] R. B. McGhee, "Some Finite State Aspects of Legged Locomotion," *Mathematical Biosciences,* vol. 2, pp. 67-84, 1968.

[7] R. B. McGhee, "Vehicular Legged Locomotion," *Advances in Automation and Robotics,* vol. 1, pp. 259-284, JAI Press Inc., 1985.

[8] R.B.McGhee and A.A.Frank, "On Stability Properties of Quadruped Creeping Gaits," *Mathematical Biosciences,* vol.3, pp.331-351, 1968.

[9] M.Russel, "Odex 1: The first functionoid," *Robotics Age*, vol.5, no.5, pp.12-18, 1983.

[10] K.J.Waldron and V.J.Vohnout, "Configuration Design of the Adaptive Suspention Vehicle," *IJRR*, vol.2, no.3, pp.37-48, 1984.

[11] S.H.Kwak and R.B.McGhee, "Rule based motion coordination for a hexapod walking machine", *Advanced Robotics*, vol.4, no.3, pp.263-282, 1990.

[12] E.Krotkov, J.Bares, T.Kanade, T.Mitchell, R.Simmons, and R.Whittaker, "Ambler: A six-legged Planetary Rover", *Proc. 5th International Conference on Advanced Robotics*, pp.717-722, 1991.

[13] Y. Sakakibara, K. Kan, Y. Hosoda, M. Hattori, and M. Fujie, "Low Impact Foot Trajectory for a Quadruped Walking Machine," *Journal of Robotics Society of Japan,* vol. 8, no. 6, pp. 22-31, December 1990, in Japanese.

[14] S. Hirose, K. Yoneda, R. Furuya, and T. Takagi, "Dynamic and Static Fusion Control of Quadruped Walking Vehicle," *Proc. IROS'89,* pp. 199-204, in Tsukuba, Japan, September 1989.

[15] Kanayama, Y., McGhee, R.B., Yoneda, K., Suzuki, K., McMillan, S., Takahashi, H., and Iwasaki, M., " An International Joint Research Project on an Autonomous Underwater Walking Robot," Proc. International Symposium on Coastal Ocean Space Utilization, in Yokohama, Japan, May 30 - June 2, pp. 181-192, 1995.

[16] J. Akizono, M. Iwasaki, T. Nemoto, and O. Asakura, "Development on Walking Robot for Underwater Inspection," *Proc. the 4th International Conference on Advanced Robotics, Springer-Verlag,* pp. 652-663, June 1989.

[17] Akizono, J., Iwasaki, M., Nemoto, T., and Asakura, O., "Field Test of Aquatic Walking Robot for Underwater Inspection," *Mechatronic Systems Engineering,* vol. 1, Kluwer Academic Publishers, pp. 233-239, 1990

[18] Kanayama, Y., Yoneda, K., Suzuki, K., McGhee, R.B., and Takahashi, H., "An International Joint Research Project on an Autonomous Underwater Walking Robot," Proc. Robot Symposium of Robotics Society of Japan, pp. 245-250, in Tokyo, May 27-28, 1994.

[19] K. Yoneda, K. Suzuki, and Y. Kanayama, "Gait Planning for Versatile Motion of a Six Legged Robot," *Proc. IEEE Int. Conf. on Robotics and Automation,* pp. 1338-1343, 1994.

[20] McMillan, S., Orin, D.E., and McGhee, R.B., "Efficient Dynamic Simulation of an Unmanned Underwater Vehicle with a Manipulator", Proc. IEEE Intl. Conf. on Robots and Automation in San Diego, California, pp. 1133-1140, May 8-13, 1994.

[21] Nelson, M.L., Byrnes, R.B., Kwak, S.H., and McGhee, R.B., "Putting Object- Oriented Technology to Work in Autonomous Vehicles", *Proc. of Tools USA '93 Conference,* Santa Barbara, CA, pp. 279-288, August, 1993.

[22] Byrnes, R.B., Nelson, M.L., Kwak, S.H., McGhee, R.B., and Healey, A.J., "Rational Behavior Model: An Implemented Tri-Level Multilingual Software Architecture for Control of Autonomous Underwater Vehicles", *Proc. of 8th Intl. Symposium on Unmanned Untethered Submersible Technology,* Univ. of New Hampshire, Durham, NH, pp.160-178, Sept., 1993.

[23] Y. Kanayama and M. Onishi, "Locomotion Functions in the Mobile Robot Language, MML," *Proc. IEEE International Conference on Robotics and Automation,* pp. 1110-1115, in Sacrament, California, April 1991.

[24] J. J. Craig, *Introduction to Robotics: Mechanics and Control, second edition,* Addison-Wesley Publishing Company, Inc., 1989.

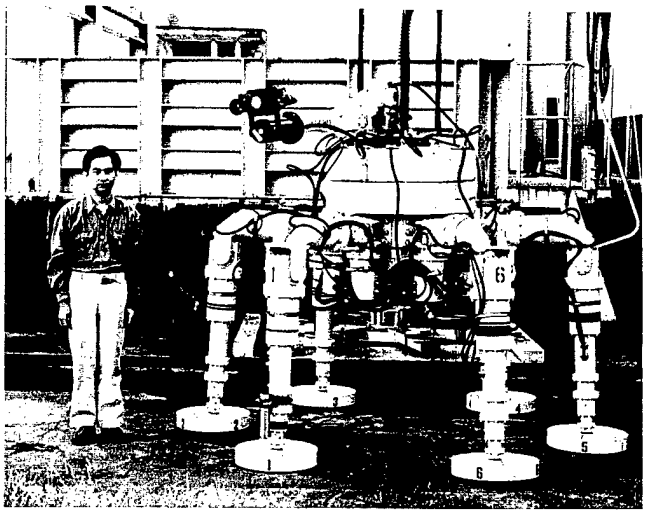

Figure 1: AQUAROBOT.

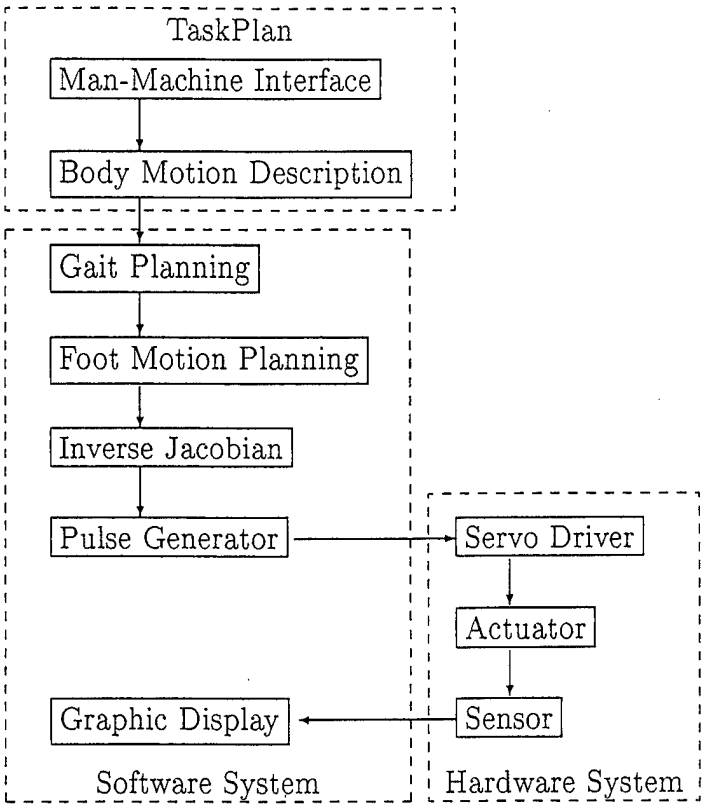

Figure 2: Control Architecture

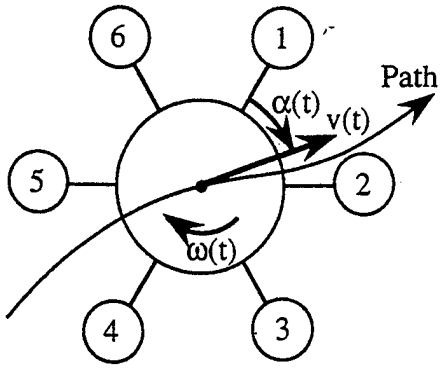

Figure 3: Motion description.

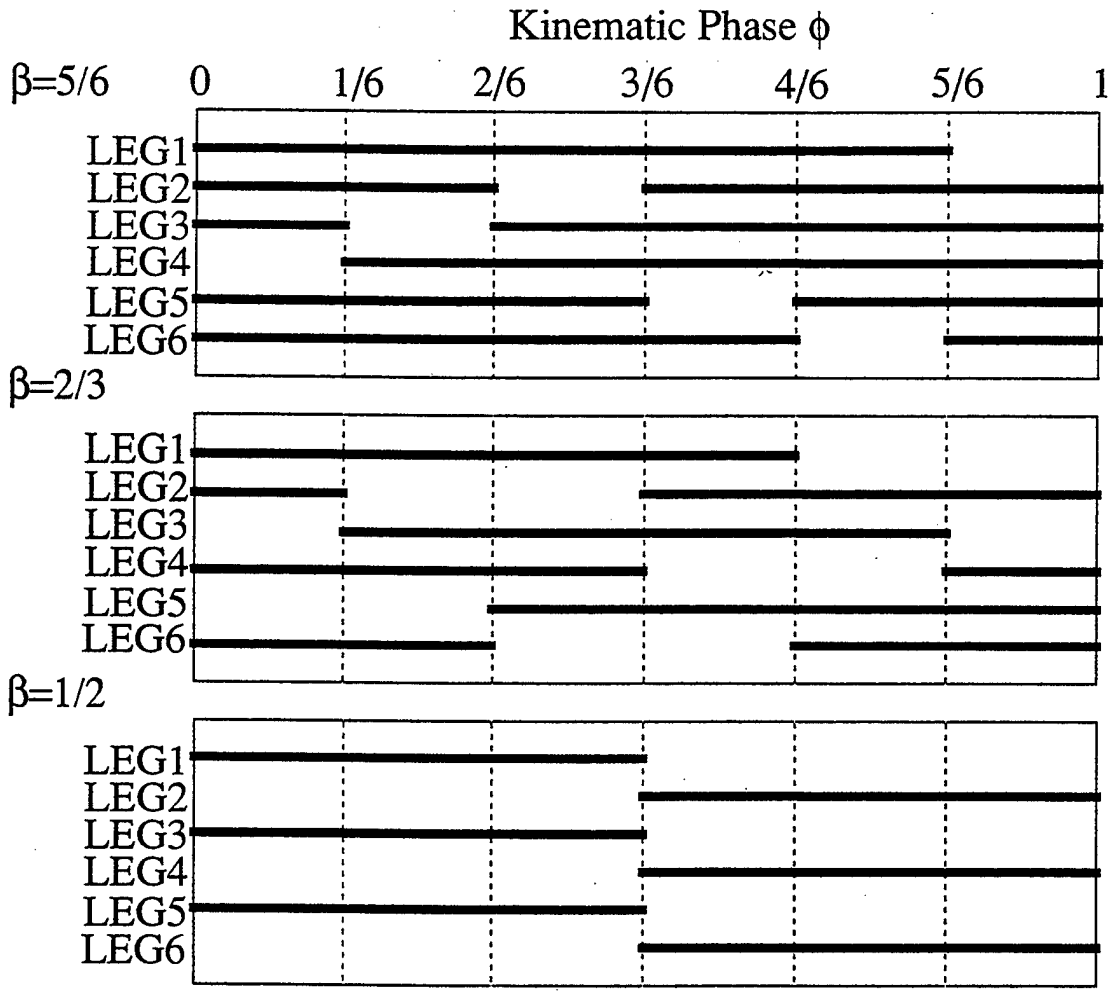

Figure 4: Gait diagrams of forward wave gaits($\alpha = \pi/6$).

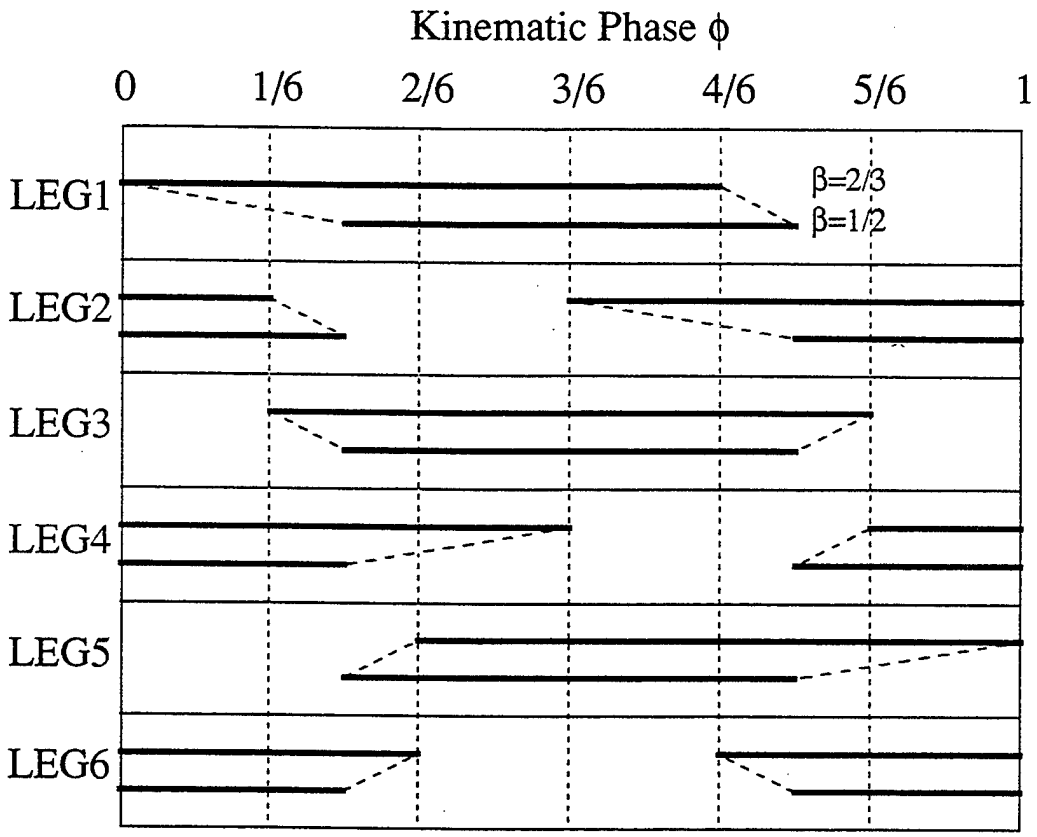

Figure 5: Gait diagram obtained by interpolation on $\beta(\alpha = \pi/6)$.

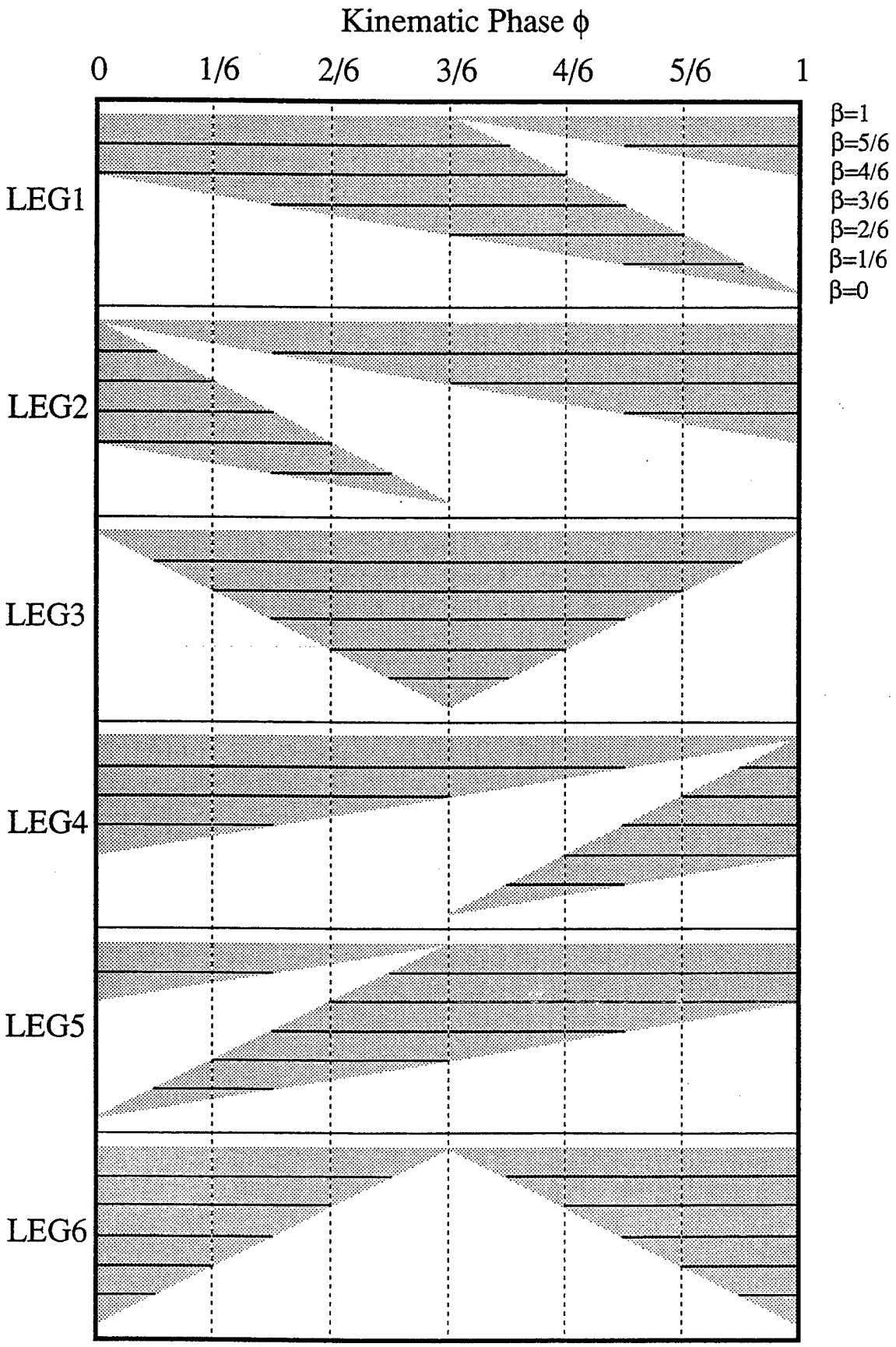

Figure 6: Gait diagram of variable duty factor wave gait with a fixed crab angle $\alpha = \pi/6$. Shaded parts represent support phase.

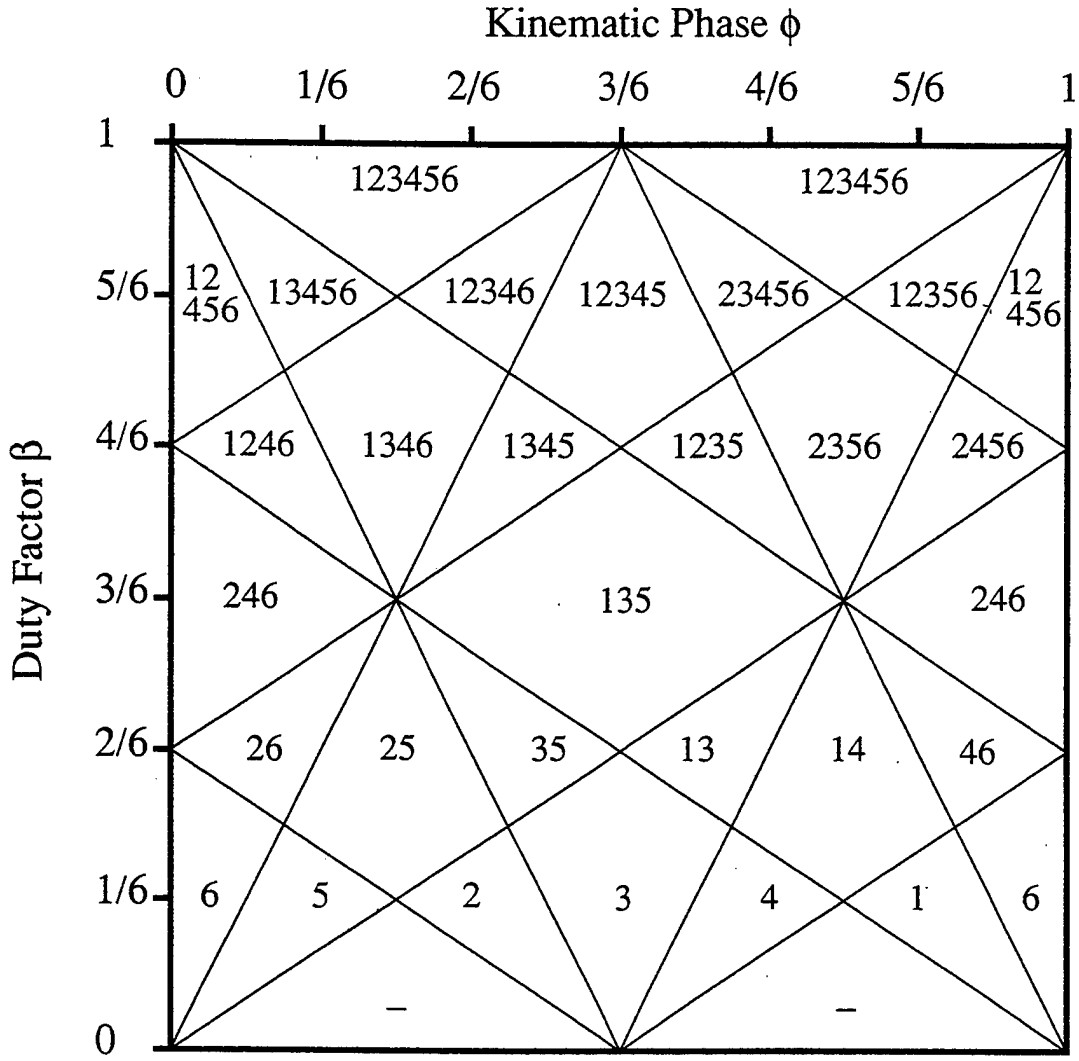

Figure 7: Supporting leg chart of variable duty factor wave gait ($\alpha = \pi/6$).

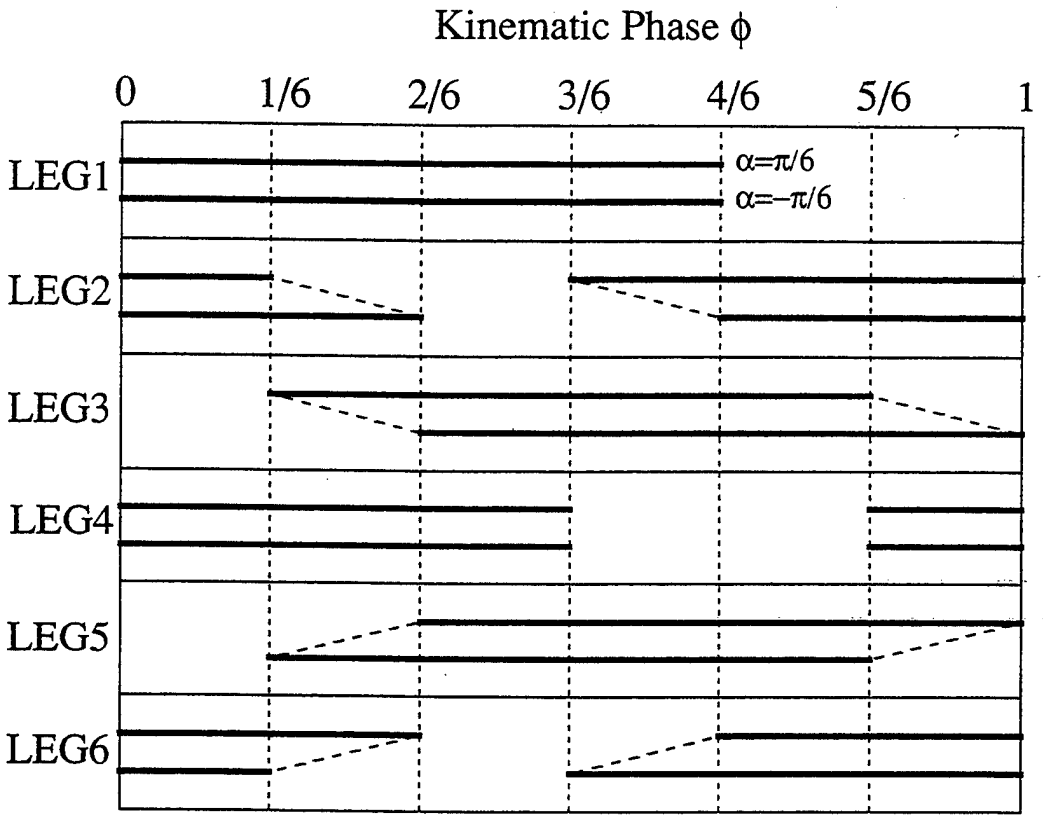

Figure 8: Gait diagram obtained by interpolation on $\alpha(\beta = 2/3)$.

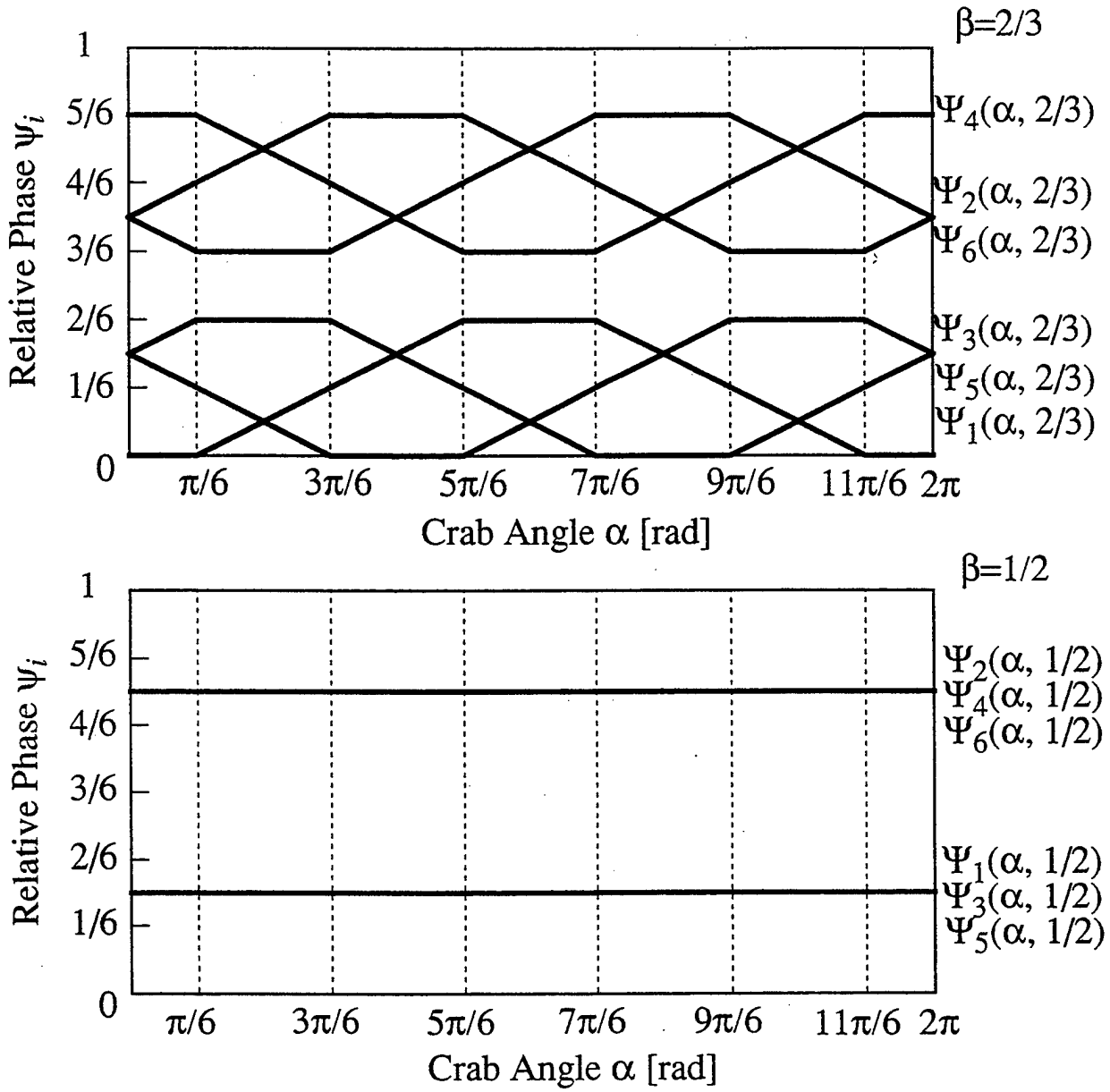

Figure 9: Relative phase at variable crab angle.

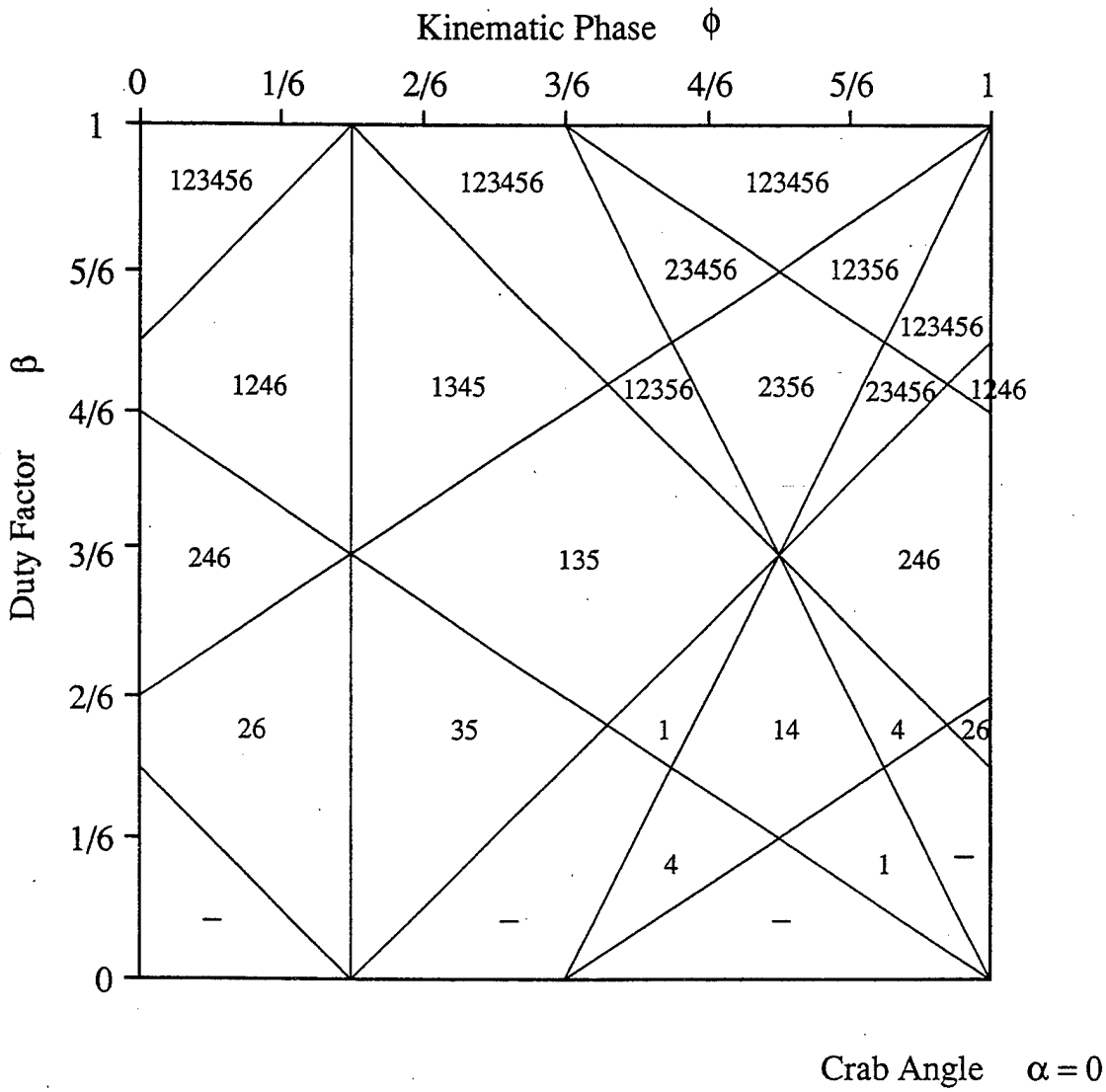

Figure 10: Supporting leg chart of variable parameter wave gait ($\alpha = 0$).

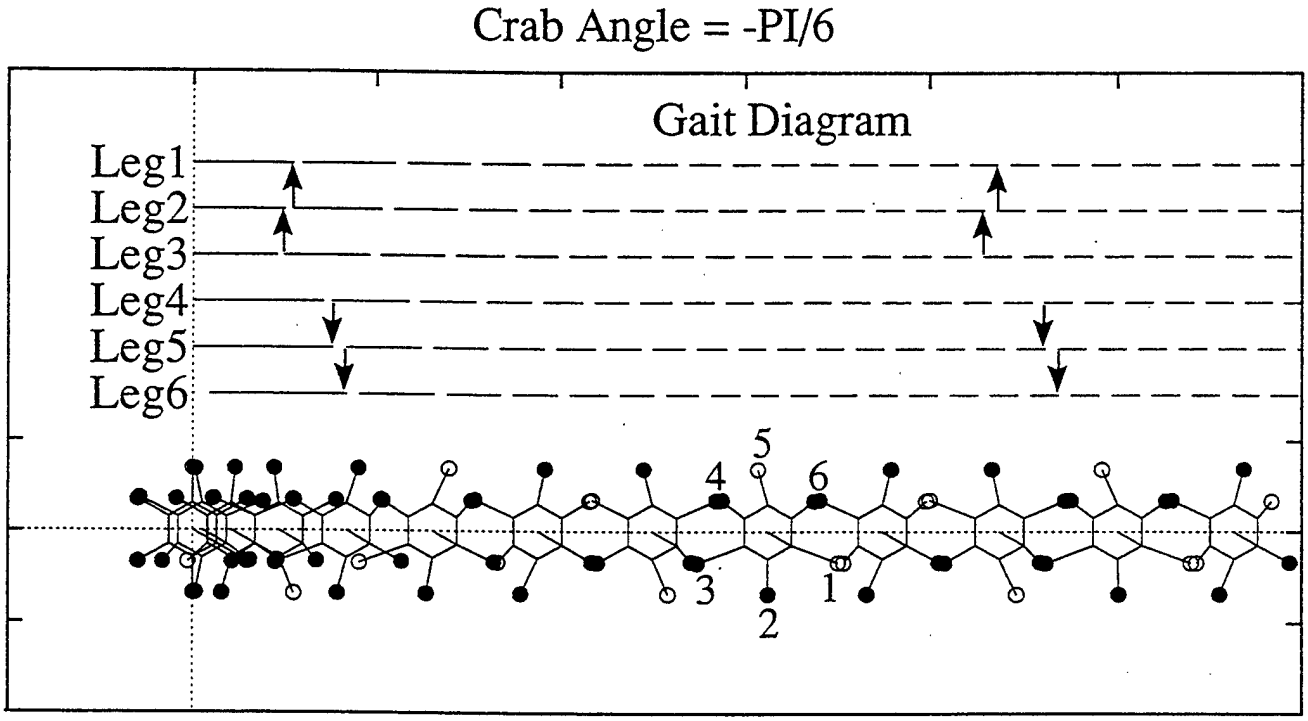

Figure 11: Example of generated gait of a constant crab angle case. The duty factor is decreasing from 1.0 (on the left) to 0.5 (on the right). The waves of lift-offs propagate as the arrows show.

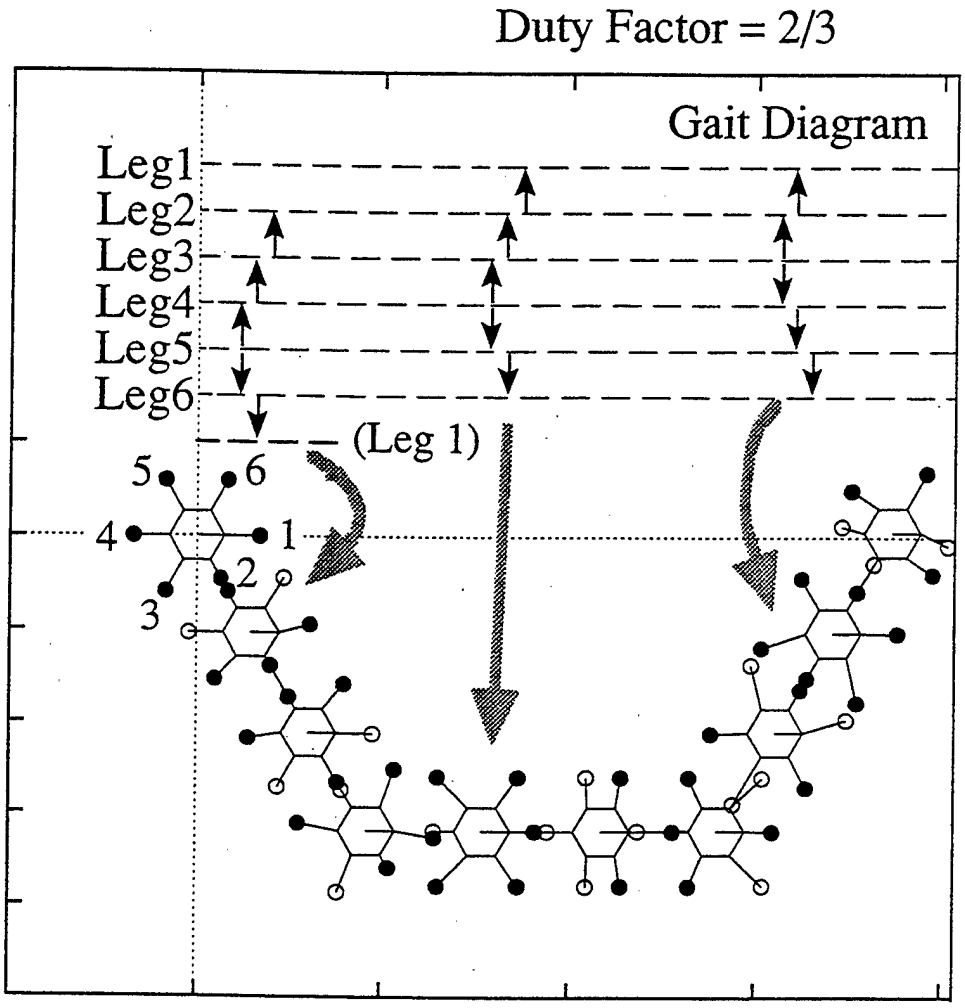

Figure 12: Example of the generated gait of a constant duty factor case. Even if the crab angle is changing, the waves of lift-offs propagate forward as the arrows show.

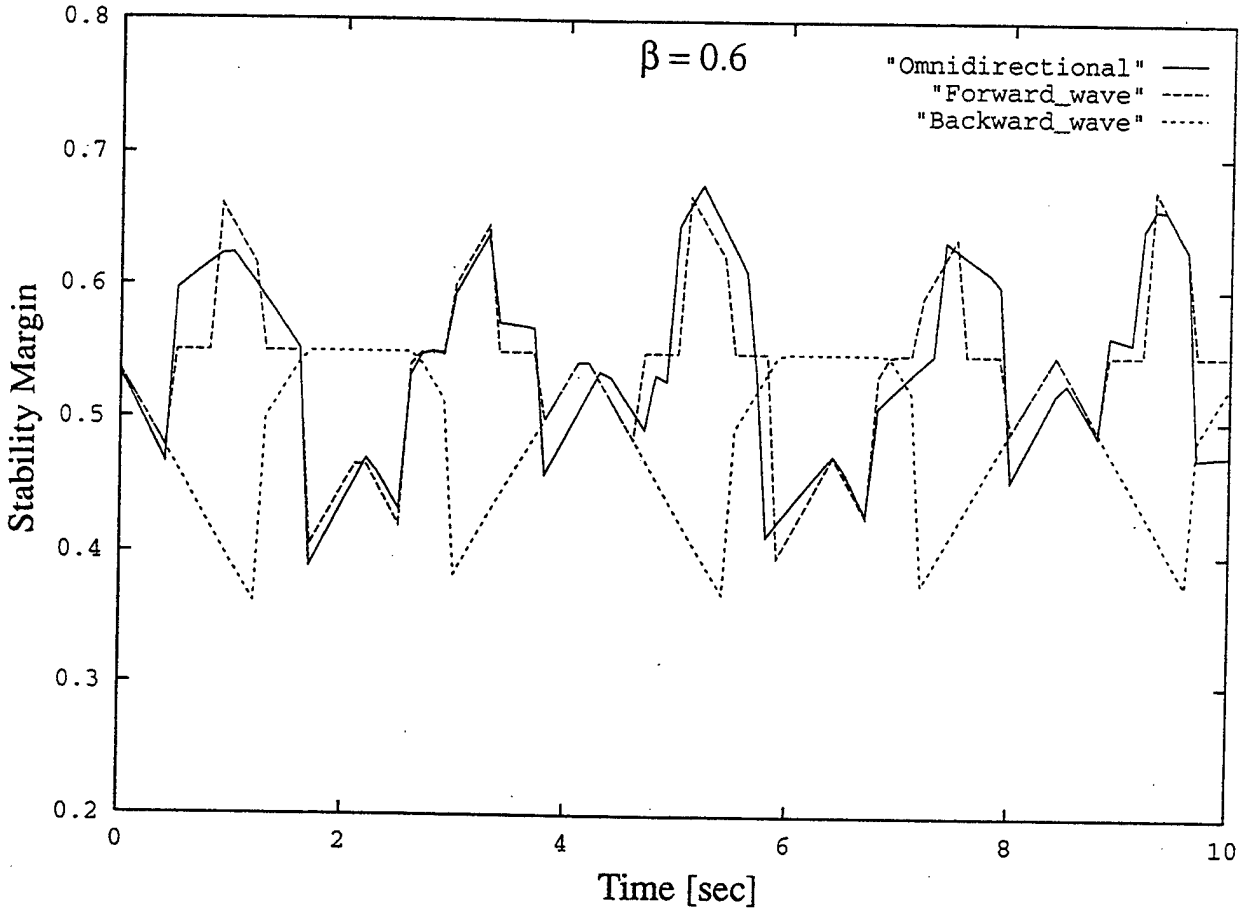

Figure 13: Comparison of stability margins. The minimum values of proposed omnidirectional gait and forward wave gait are significantly larger than that of backward wave gait.

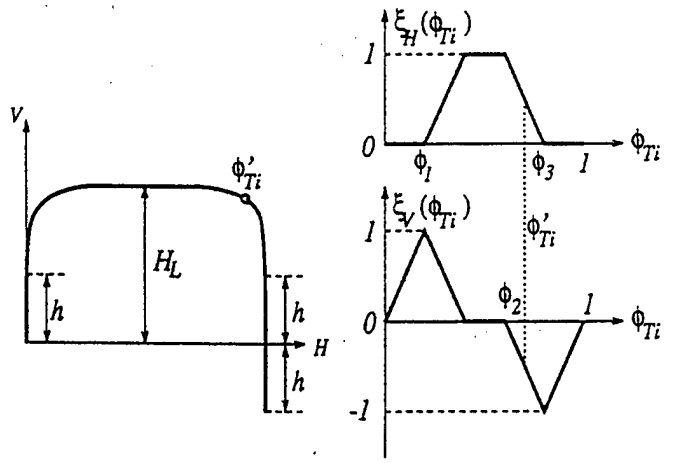

(a) Trajectory Plane (b) Velocity Template

Figure 14: Trajectory template.

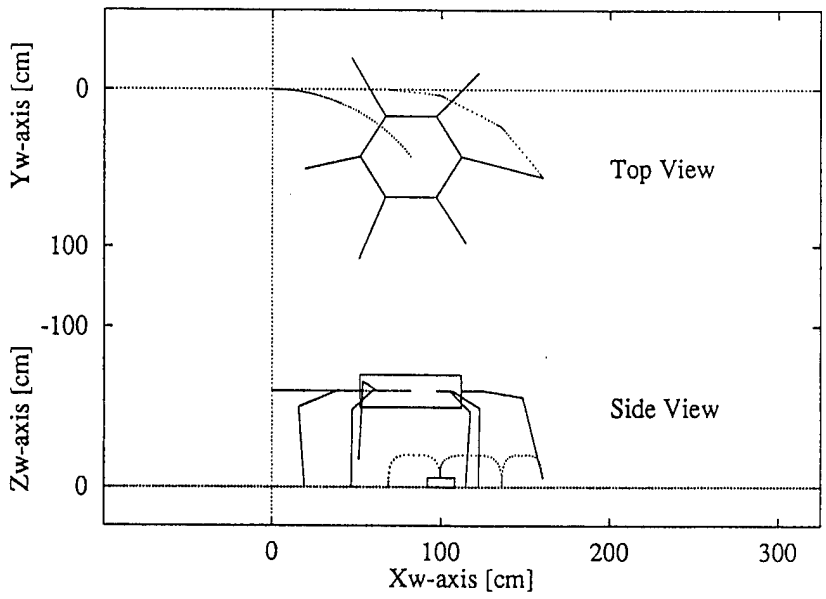

Figure 15: Simulation of the foot motion planning. The robot is stepping over an obstacle.

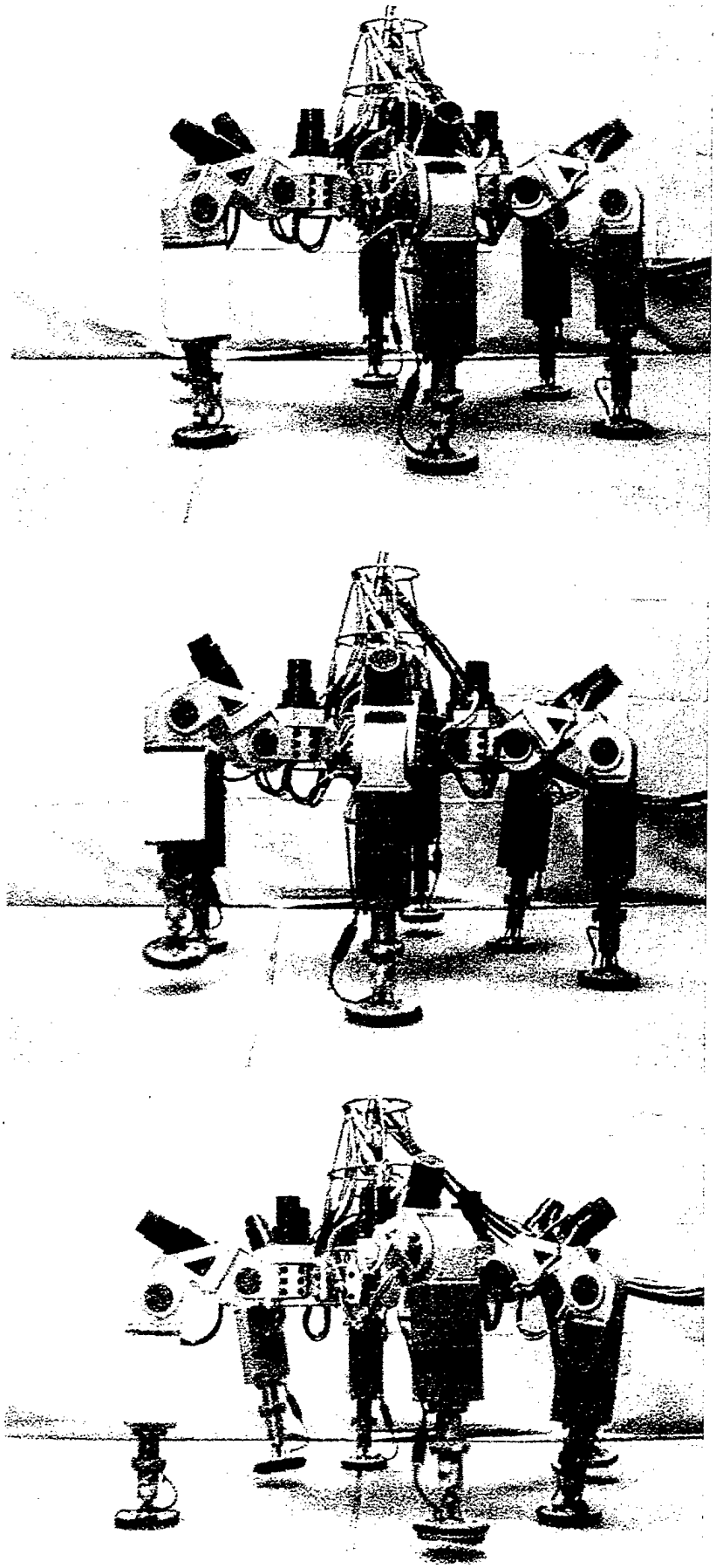

Figure 16: Experiment of variable duty factor walk. The number of swing leg is changing.

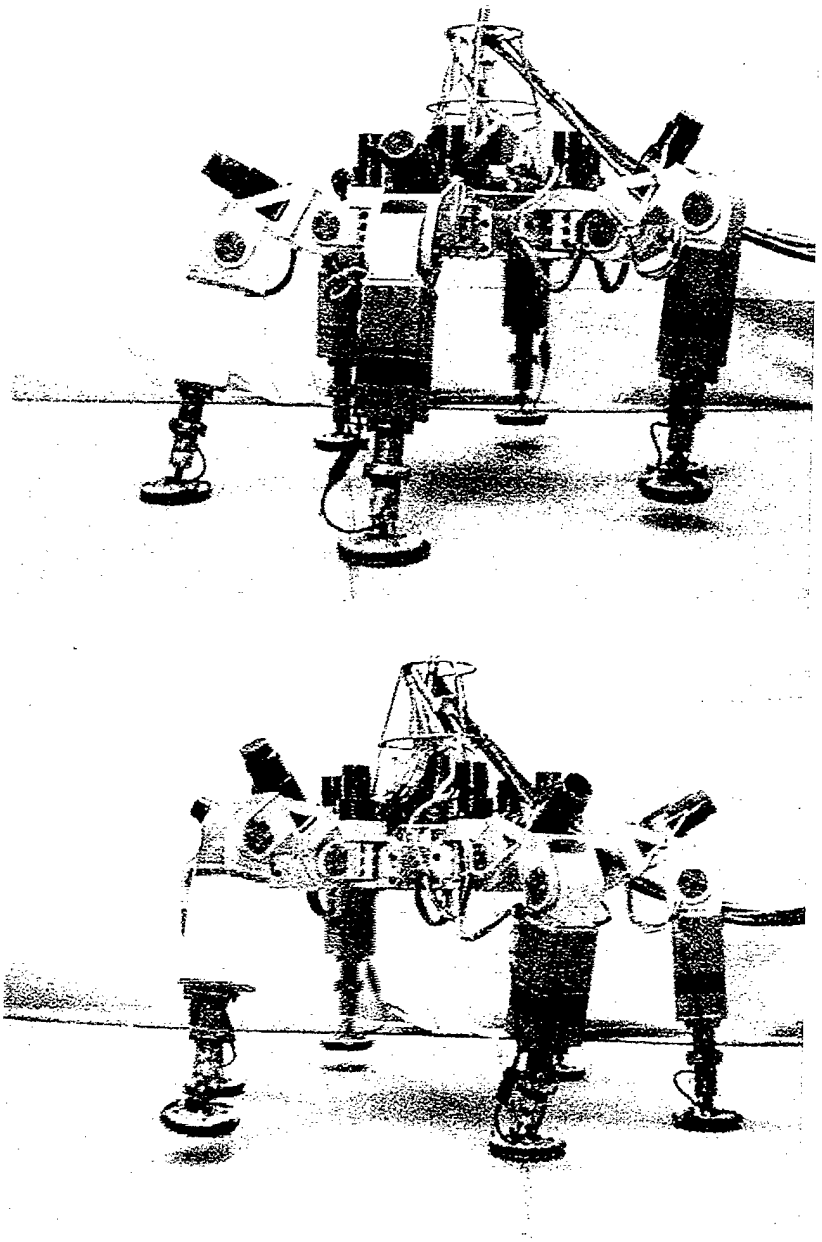

Figure 17: Experiment of variable crab angle walk. The combination of swing leg is changing.

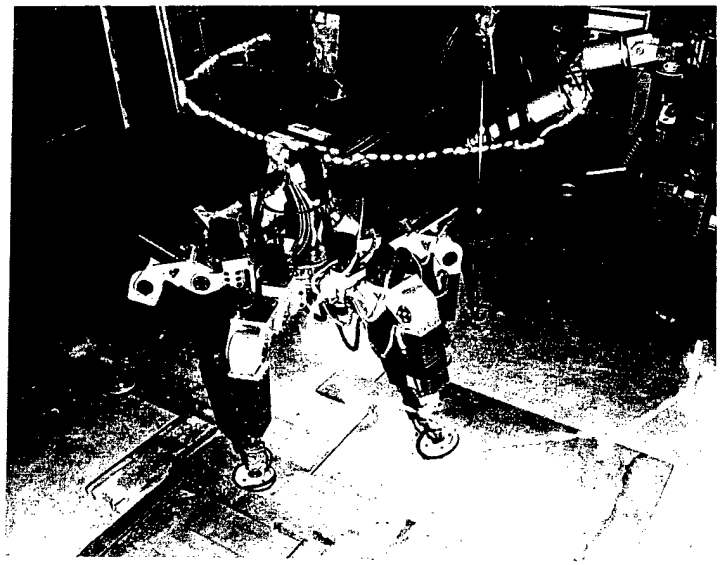

Figure 18: Walking over obstacle. Broken lines indicate the trajectory of the body and leg.

INITIAL DISTRIBUTION LIST

1.	Defense Technical Information Center 8725 John J. Kingman Rd., STE 0944 Ft. Belvoir, VA 22060-6218	2
2.	Dudley Knox Library Naval Postgraduate School Monterey, CA 93943-5100	2
3.	Research Office, Code 09 Naval Postgraduate School Monterey, CA 93943-5100	1
4.	Jun'ichi Akizono Robotics Laboratory, Machinery Division Port and Harbour Research Institute Ministry of Transport 3-1-1 Nagase, Yokosuka 239 Japan	6
5.	Norman Caplan Biological and Environmental Systems National Science Foundation 1800 G Street, N.W. Washington, D.C. 20550	1
6.	Shuichi Itoh Department of Electronics Engineering The University of Electro-Communications 1-5-1 Chofugaoka, Chofu 182 Japan	1
7.	Yutaka Kanayama Department of Computer Science Naval Postgraduate School Monterey, CA 93943	10
8.	Robert McGhee Department of Computer Science Naval Postgraduate School Monterey, CA 93943	1

9. Scott McMillan — 1
908 Beacon Square Court #320
Gaitherburg, MD 20878

10. Yutaka Nagai — 1
Department of Electronics Engineering
The University of Electro-Communications
1-5-1 Chofugaoka, Chofu 182 Japan

11. Daisuke Ookane — 1
Kobayashi Lab. Precision Engineering Department
Meiji University
1-1-1 Higashi-mita, Tama-ku
Kawasaki 214 Japan

12. David Orin — 1
Department of Electrical Engineering
2015 neil Avenue
Columbus, OH 43210

13. Charles Schue — 1
209 E. Vineyard Ct.
Cape May, NJ 08204

14. Kenji Suzuki — 10
Control Systems Lab., Hiroshima R&D Center
Mitsubishi Heavy Industries, Ltd.
4-6-22 Kan'on-shin-machi, Nishi-ku
Hiroshima 733 Japan

15. Hidetoshi Takahasi — 4
Yokohama Machinery Improvement Office
Second District Port Construction Bureau
Ministry of Transport
2-1-4 Hashimoto-cho, Kannagawa-ku
Yokohama 231 Japan

16. Tomoyoshi Takeuchi — 1
Department of Electronic Engineering
The University of Electro-Communications
1-5-1 Chofugaoka, Chofu 182 Japan

17. Toshimichi Tsumaki — 1
Electronics Equipment Division
Research and Development Department
Sagamihara Machinery Works
Mitsubishi Heavy Industries LTD.
3000 Tana, Sagamihara-shi
Kanagawa-ken 299 Japan

18. Ura Tamaki — 1
Institute of Industrial Science
University of Tokyo
7-22-1 Roppongi, Minato-ku
Tokyo 106 Japan

19. Kan Yoneda — 20
Department of Mechano-Aerospace Engineering
Tokyo Institute of Technology
2-12-1 Ookayama, Meguro, Tokyo 152 Japan

20. Xiaoping Yun — 1
Department of Electrical and Computer Engineering
Naval Postgraduate School
Monterey, CA 93943